Materials in Regenerative Medicine

Mater. Res. Soc. Symp. Proc. Vol. 1140 © 2009 Materials Research Society 1140-HH01-02

Dual and Triple Shape Capability of AB Polymer Networks Based on Poly(ε-caprolactone)dimethacrylates

Marc Behl[1], Ingo Bellin[2], Steffen Kelch[3], Wolfgang Wagermaier[1] and Andreas Lendlein
[1]Institute of Polymer Research, GKSS Research Centre GmbH, Kantstr. 55, 14513 Teltow, Germany
[2]Global Polymer Research – Foams, BASF Aktiengesellschaft, GKT/F - B 001, 67056 Ludwigshafen, Germany
[3]Sika Technology AG, Tüffenwies 16, CH-8048 Zürich, Switzerland

ABSTRACT

Shape-Memory polymers are an emerging class of functionalized materials, which are able to change their change in a predefined way upon appropriate stimulation. In the past research has mostly focused on the implementation of new ways to trigger the shape-memory effect. Although the stimuli were differing, these systems were dual-shape materials. Recently, multi-phase shape-memory polymers with an additional switching phase were introduced. These materials allow the selection of the switching segment according to the requirements of the specific application. The dual shape-capability and the underlying molecular mechanisms are discussed for such multiphase polymer networks. Furthermore, these materials display triple-shape capability after appropriate programming, which enables them to change from a first shape (A) to a second shape (B) and from there to a third shape (C). Two different polymer network architectures for triple-shape polymer networks are described and investigated towards their dual and triple shape-properties. The programming of these materials can be fairly complex, therefore we will show finally an one-step programming to reach triple-shape capability.

INTRODUCTION

Shape-memory polymers have received considerable interest because of their ability to change their shape in a predefined way from a shape (A) to a shape (B) upon appropriate stimulation. This stimulation has been realized either by heat [1] or light [2]. Indirect actuation of the shape-memory effect was realized by application of irradiation with IR-light [3], of electrical fields [4], exposure to alternating magnetic fields [5, 6] or immersion in water [7]. Thus far, these systems were all dual-shape materials.
Recently, thermally-induced shape-memory polymers with an additional switching phase have been introduced [8], allowing the predefined movement by gradual temperature increase from a shape (A) to a shape (B) at a switching temperature which is determined by either the lower or the higher thermal transition. A prerequisite for this general concept is a polymer network structure with at least two phase separated domains which act as physical crosslinks. These domains have individual transition temperatures (T_{trans}), which are, depending on the type of chain segment, either a glass transition temperature (T_g) or a melting temperature (T_m). Upon cooling below T_{trans} of a specific domain, the domain solidifies and forms physical cross-links. As these additional cross-links dominate the covalent netpoints, they offer the temporary fixation of a new

shape, which can be recovered into its original shape when being reheated above T_{trans}. By deformation of the polymer network and subsequent cooling in the deformed shape, this effect is used in dual-shape materials for the temporary fixation of a second shape. While shape (B) is given by the covalent crosslinks during polymer network formation, shape (A) is fixed by physical crosslinks created in a one-step thermomechanical programming process. In this programming process shape (A) is temporarily fixed by one of the two switching domains.

EXPERIMENT

Synthesis of the materials is described in references [8-10].

Cyclic, Thermomechanical Experiments. These were carried out on a Zwick (Ulm, Germany) Z005 for *CLEG*-networks and a Zwick Z1.0 for *MACL*-networks equipped with thermochambers controlled by Eurotherm control units (2216E for Z005 and 2408 for Z1.0, Eurotherm Regler, Limburg, Germany). The thermochamber for the Z005 was a T35 provided by Mytron (Heiligenstadt, Germany) while for the Z1.0 a thermochamber W91255 designed by Zwick was used. In both cases cooling was realized by a gas flow from a liquid nitrogen tank. 200 N, 100 N, and 20 N load cells were used depending on samples and temperature. Films were cut into standard samples (ISO 527-2/1BB) and strained at an elongation rate of 10 $mm \cdot min^{-1}$.

In a triple shape experiment (Fig. 1) the sample is stretched at T_{high} = 70 °C for CLEG and T_{high} = 150 °C for MACL networks from ε_C, where the elongation corresponds to shape (C), to ε_B^0. Cooling with a cooling rate (β_c) of 5 $K \cdot min^{-1}$ to T_{low} = -10 °C for CLEG or T_{low} = 0 °C for MACL networks under stress-control results in ε_{Bload}. Afterwards the sample is held unloaded at T_{low} for 10 min. Subsequently the sample is heated to T_{mid} and after passing T_{sw} with some additional time for equilibration at T_{mid} which was in case CLEG networks 40 °C with a heating rate of β_h = 2 $K \cdot min^{-1}$ and in case of MACL networks 70 °C with a heating rate of β_h = 5 $K \cdot min^{-1}$ ε_B is reached, which is shape (B). The sample is further stretched to ε_A^0 and cooled to T_{low} under stress-control with β_c = 5 $K \cdot min^{-1}$, whereas the elongation decreases to ε_{Aload}. Shape (A), corresponding to ε_A, is obtained by unloading after 10 min for *CLEG*-networks and 30 min for MACL networks. The recovery process of the sample is monitored by reheating with a heating rate of 1 $K \cdot min^{-1}$ from T_{low} to T_{high} while the stress is kept at 0 MPa. The sample contracts to recovered shape (B) at ε_{Brec}, which is defined as the elongation at the minimum contraction rate. Continued heating finally leads to recovery of shape (C) at ε_{Crec}. This cycle is conducted five times with the same sample.

DISCUSSION

This concept was realized in polymer network architecture, in which poly(ε-caprolactone)dimethacrlyate (PCLDMA) was copolymerized with poly(ethyleneglycol)monomethylethermethacrylate (PEGMA). These graft polymer networks are named CLEG. In such a polymer network the elasticity is mainly determined by the PCL segments which are crosslinking short polymethacrylate segments having dangling poly(ethyleneglycolmonomethylether) (PEG) segments. In CLEG networks three situations for dual shape fixation can be differentiated depending on the switching temperature [9]. I) Use of the crystallization of PCL phase for fixation of the temporary shape. II) Crystallization of the pendant PEG chain segments prevents the amorphous PCL segments from returning into the coiled state. III) Both segments can contribute

to the fixation of a temporary shape. At first PCL chain segments crystallize followed by the crystallization of the PEG segments. It was shown, that every sample returns to its permanent shape, as soon as the switching temperature T_{sw} is exceeded, which is the experimentally determined temperature at the inflection point of the recovery curve. As expected, T_{sw} is close to T_m(PEG) for case II and close to T_m(PCL) for case I and III. As the material possesses two independent transition temperatures $T_{trans,\,A}$ and $T_{trans,B}$ it could also be shown that the material has triple-shape capability [8]. It should be noted that not every material presenting two independent transition temperatures displays triple shape-capability.

Triple-shape materials are materials that are able to change from a first shape (A) to a second shape (B) and from there to a third shape (C). For investigating the generality of the triple-shape capability a second multiphase polymer network was explored. In this polymer network system, called MACL, cyclohexylmethacrylate (CHMA) and PCLDMA were copolymerized. Here the polymer network structure is build by the PCLDMA and the polymerized CHMA segments. Both segments are contributing equally to the overall elasticity of the polymer network structure. In this polymer network $T_{trans,A}$ is given by the T_g of the MACL and $T_{trans,B}$ by the T_m of the PCL segments.

The triple-shape-memory effect can be characterized in specific cyclic thermomechanical experiments. In a two-step uniaxial deformation experiment the two additional shapes A and B are programmed. Afterwards, when the sample is reheated, shape B and finally shape C are recalled. These cyclic thermomechanical experiments allow the quantification of the triple-shape effect for each shape separately. While the shape fixity ratio [R_f(X→Y)] describes the ability to fix shape Y after the thermomechanical programming, the shape recovery ratio [R_r(X→Y)] is a measure to what extent shape Y can be recovered starting from shape X.

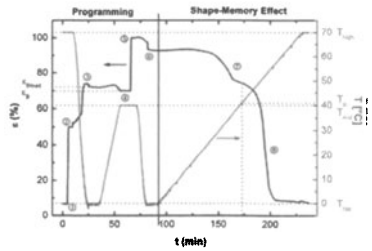

Figure 1. Cyclic, thermomechanical experiment of CL(40)EG (fifth cycle) as a function of time; solid line, strain; dashed line, temperature.

The programming of these materials can be done by different methods. Previously shown programming method I involves the stretching of the sample at T_{high} from ε_C, where the elongation corresponds to shape (C), to ε_B^0. Cooling to T_{mid} under stress-control results in ε_{Bload}. Unloading leads to ε_B, which is shape (B). The sample is further stretched to ε_A^0 and cooled to T_{low} under stress-control, whereas the elongation decreases to ε_{Aload} and shape (A), corresponding to ε_A, is obtained by unloading [8]. In contrast, a newly presented programming method II starts with stretching the sample at T_{high} from ε_C, where the elongation corresponds to shape (C), to ε_B^0. Cooling to T_{low} under stress-control results in ε_{Bload}. Afterwards the sample is held unloaded at T_{low} for 10 min. Subsequently the sample is heated to T_{mid} and after passing T_{sw} with some addi-

tional time for equilibration at T_{mid} ε_B is reached, which is shape (B). Then the sample is strained to ε_A^0. Cooling down to T_{low} leads to a decrease of the elongation because of the crystallization of the PEG segments. After unloading the sample is held at T_{low} for 10 min whereas shape (A) is obtained. Finally, after both programming methods, the sample is heated to T_{high}. A typical stress strain diagram for a CLEG polymer network is displayed in Fig. 2. The average values for the 2nd to 5th cycle of both polymer network architectures, which all exhibit the triple shape effect, are presented in table 1. The first cycle is not considered for the calculation, as this cycle is needed for the equalization of the thermomechanical history of the samples.

Table 1 Triple shape properties of polymer networks programmed with programming method II

polymer network †	ε_B^0 [%]	ε_A^0 [%]	$\overline{R}_f$ (C→B) [%] §	$\overline{R}_f$ (B→A) [%] §	$\overline{R}_r$ (A→B) [%] §	$\overline{R}_r$ (A→C) [%] §
CL(30)EG	50	100	96.8 ± 0.4	91.2 ± 0.9	82.9 ± 4.4	98.9 ± 0.8
CL(40)EG	50	100	96.6 ± 0.3	83.4 ± 1.1	77.5 ± 1.4	99.1 ± 0.6
CL(40)EG	70	100	97.2 ± 0.2	91.1 ± 1.2	90.0 ± 3.0	100.0 ± 0.9
CL(40)EG	50	120	97.5 ± 0.5	95.2 ± 1.4	84.1 ± 1.0	98.6 ± 0.8
CL(50)EG	50	100	97.5 ± 0.2	84.5 ± 2.4	73.1 ± 1.8	98.5 ± 0.1
CL(60)EG	50	100	97.6 ± 0.8	75.7 ± 1.1	-	106.0 ± 0.9
MACL(40)	50	100	96.9 ± 1.1	97.9 ± 0.4	74.7 ± 2.4	96.6 ± 4.1
MACL(45)	50	100	96.9 ± 0.6	98.7 ± 0.1	97.0 ± 1.0	97.3 ± 1.8
MACL(50)	50	100	97.0 ± 0.3	98.9 ± 0.1	101.4 ± 1.2	100.7 ± 2.5
MACL(60)	50	100	96.5 ± 0.2	99.3 ± 0.1	102.9 ± 0.7	100.0 ± 2.4

† the number in brackets indicates the content of PCL in wt%
§ average of cycles 2-5, values higher 100.0 are artefacts resulting from the tensile tester

The following equations were used to characterize the triple-shape effect.

$$R_f(X \rightarrow Y) = (\varepsilon_y - \varepsilon_x) / (\varepsilon_{yload} - \varepsilon_x) \quad (1)$$

$$R_r(X \rightarrow Y) = (\varepsilon_x - \varepsilon_{yrec}) / (\varepsilon_x - \varepsilon_y) \quad (2)$$

In CLEG networks R_f(C→B) increases with increasing PCL content as this supports the fixation of shape A, but goes along with a decrease of R_f(B→A). In contrast in MACL networks having triple shape capability R_f(C→B) does not show an influence of PCHMA content and also R_f(B→A) remains on a high level. This has been attributed to the difference in the network architecture, as in CLEG networks the overall elasticity is only determined by the PCL segments, while in MACL networks both segments contribute to the elasticity. All triple-shape memory materials show almost complete total recovery R_r(A→C). In comparison to CLEG networks the values for R_r(A→B) are higher in MACL networks and increase with growing PCL content. In contrast in CLEG networks R_r(A→B) decreases with increasing PCL content and has been explained by additional strain –induced crystallization of amorphous PCL. For MACL(50) and MACL(60) networks a complete recovery of the first temporary shape could be observed, while networks with less content of PCL show an incomplete recovery of the first shape. The compari-

son of the results from programming method I with the programming here presented, turns out that for CLEG and MACL with programming method II higher values of R_f(C→B) can be reached while R_f(B→A) is slightly lower or constant. In contrast, values of R_f(A→B) of CLEG networks are higher for networks with more than 40 wt% PCL with programming method II and higher for networks with less than 40 wt% PCL with programming method I. In MACL networks values for R_f(A→C) are similar with both programming methods while values for R_f(A→B) are higher for networks of more than 45 wt% PCL with programming method II.

As the programming to achieve the triple shape capability is quite complex and is even more time consuming with programming method II a one step programming method was developed [10]. This requires a polymer network architecture where both switching segments contribute to the overall elasticity as given in MACL networks. Here at T_{high} = 150 °C both chain segments are flexible, at T_{mid} = 70 °C the PCHMA chain segments are in the glassy state and upon further cooling to -10 °C the PCL chain segments form stiff flexible amorphous and rigid crystalline phases. Similar to the programming of a triple shape material for a dual shape effect [9], the samples can also be programmed in three different temperature ranges: case I T_{low} = 70 °C and T_{high} = 150 °C, case II T_{low} = -10 °C and T_{high} = 70 °C and case III T_{low} = -10 °C and T_{high} = 150 °C. The stress/strain experiments from theses three different programming procedures are depicted in figure 2 for MACL networks with 50 wt% PCL.

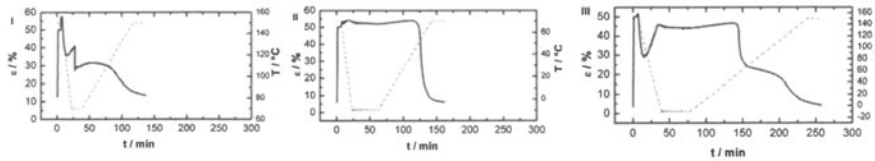

Figure 2. Strain/time diagrams (fourth cycle) obtained from cyclic, thermomechanical experiments for MACL(50): **I**: T_{low} = 70 °C and T_{high} = 150 °C; **II**: T_{low} = -10 °C and T_{high} = 70 °C; **III**: T_{low} = -10 °C and T_{high} = 150 °C.

While case I represents the dual shape capability of the PCHMA phase, case II displays the dual shape experiment for the PCL phase. When the samples were heated to T_{high} the recovery process occurs. As the time interval, which is proportional to the temperature, is significantly smaller in case II compared to case I, it can be concluded, that the melting of the PCL segments takes place over a smaller temperature interval than the softening of the PCHMA segments. In case III where both segments contribute to the fixation of the temporary shape an increase of strain, because of the thermal expansion of the sample and at 54 °C a slight decrease of the strain can be determined. This decrease has been attributed to the melting of the PCL crystallites fixing in a small amount the temporary shape. In MACL networks with 50 wt% PCL the fraction of the fixed temporary shape is considerably higher than in MACL networks with 45 wt% PCL. The recovery curves of MACL(40) for ε_m = 30, 50, 75, 100 and 125 % are displayed in figure 3a. While for ε_m = 30 % and 50 % between 0.5 and 2.0 % of the temporary shape is fixed by the PCL segments, for larger deformations (ε_m > 75 %) a plateau of about 3.5 % is reached (figure 3b). This has been attributed to the polymer network architecture, in which the PCL segments are acting as crosslinker and PCHMA segments form the backbone and therefore can be uncoiled to a larger extent, which can not be fixed by the PCL segments.

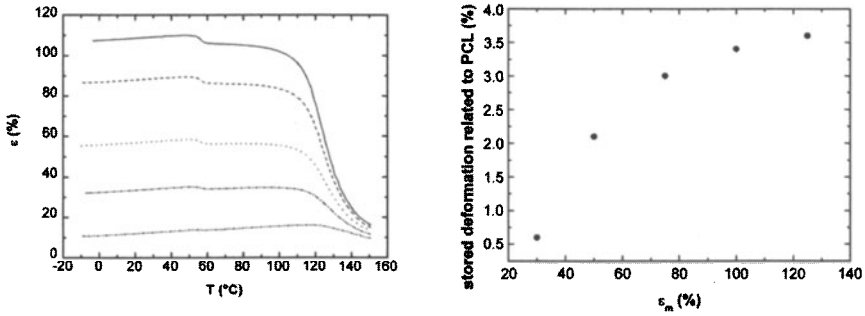

Figure 3. a Recovery curves obtained from stress-controlled, thermomechanical experiments for MACL(40) programmed with different mechanical deformations ε_m (second cycle); solid line: ε_m = 125%; dashed line: ε_m = 100%; dotted line: ε_m = 75%, dash-dotted line ε_m = 50%, dash-dot-dotted line ε_m = 30%. **b** Relationship of stored deformation of shape B to applied deformation.

CONCLUSIONS

Triple-shape materials are highly interesting materials. Proper use of programming temperature additionally enhances the versatility of these materials. Depending on the temperature used for programming either dual-shape properties with two different T_{switch} or triple-shape properties can be realized. Furthermore, by the selective choice of an appropriate programming, the triple-shape properties of such materials can be even improved, depending on the underlying molecular architecture. But this programming can be fairly complex. In certain triple-shape polymer network architecture a one-step programming was shown to be successful. A field which require complex movements of materials, e.g. for minimally invasive surgery or smart medical devices is the field of medical applications, thus seems to be very promising.

REFERENCES

1. A. Lendlein, S. Kelch, *Angew Chem, Int Ed Engl* **2002**, *41*, 2034.
2. A. Lendlein, H. Y. Jiang, O. Jünger, R. Langer, *Nature* **2005**, *434*, 879.
3. H. Koerner, G. Price, N. A. Pearce, M. Alexander, R. A. Vaia, *Nat Mater* **2004**, *3*, 115.
4. J. W. Cho, J. W. Kim, Y. C. Jung, N. S. Goo, *Macromol Rapid Commun* **2005**, *26*, 412.
5. R. Mohr, K. Kratz, T. Weigel, M. Lucka-Gabor, M. Moneke, A. Lendlein, *Proc Natl Acad Sci U S A* **2006**, *103*, 3540.
6. P. R. Buckley, G. H. McKinley, T. S. Wilson, W. Small, W. J. Benett, J. P. Bearinger, M. W. McElfresh, D. J. Maitland, *IEEE Trans Biomed Eng* **2006**, *53*, 2075.
7. B. Yang, W. M. Huang, C. Li, C. M. Lee, L. Li, *Smart Materials & Structures* **2004**, *13*, 191.
8. I. Bellin, S. Kelch, R. Langer, A. Lendlein, *PNAS* **2006**, *103*, 18043.
9. I. Bellin, S. Kelch, A. Lendlein, *J Mater Chem* **2007**, *17*, 2885.
10. M. Behl, I. Bellin, S. Kelch, A. Lendlein, *Adv Funct Mater* **2009**, *19*, 102.

Mater. Res. Soc. Symp. Proc. Vol. 1140 © 2009 Materials Research Society 1140-HH07-02

Bioreactor Systems in Regenerative Medicine: From Basic Science to Biomanufacturing

Elia Piccinini, David Wendt, Ivan Martin
Institute for Surgical Research and Hospital Management, University Hospital Basel, Hebelstrasse 20, 4031 Basel, Switzerland

ABSTRACT

In recent years, 3D culture models have started showing their extensive potential as one of the strategic tools in the fields of tissue engineering and regenerative medicine to study various aspects of cell physiology and pathology, as well as to manufacture cell-based grafts. Given the crucial role that bioreactors play in establishing a comprehensive level of monitoring and control over specific environmental factors in 3D cultures, we review herein some of the manifold possibilities correlated with bioreactor systems in the transitional pathway between the bench and the bedside. In particular, we will draw the attention to their functions as: *1) 3D culture model systems*, enabling to outline specific aspects of the actual *in-vivo* milieu and, when properly integrated with *computational modelling* and *sensing and control* techniques, to address challenging scientific questions; *2) Graft manufacturing devices*, implementing bioprocesses so as to support safe, standardized, scaleable, traceable and possibly cost-effective production of grafts for pre-clinical and clinical use.

INTRODUCTION

Bioreactors are generally regarded as devices used in industrial biotechnological processes in order to provide a defined and controlled environment to a biological source. In Tissue Engineering (TE) applications, a "bioreactor" was initially a simple Petri dish undergoing mixing and incubated at a controlled temperature. Over time, the evolution of technical tools and the need of a better comprehension of cellular mechanisms have lead to the development of more sophisticated *in vitro* systems.

Quite recently, bioreactors have shown to be able to overcome limitations of conventional manual methods (e.g., seeding of cells into porous scaffolds and maintenance in culture of the resulting engineered constructs) to drive the development of structurally defined and functionally effective engineered grafts. In addition, bioreactors constitute technological instruments to perform controlled studies aimed at understanding the effects of biological, chemical or physical cues on cells behavior in a 3D engineered construct by maintaining specific parameters within defined ranges. These attractive features give bioreactors the capability to play an active role in facilitating the entry of TE products in the market of clinical products, or to be a new kind of product by themselves.

Defining an adequate correspondence between clinical efficacy and overall costs of TE products is one of the most strategic challenges still to address to successfully translate TE technology from bench to bedside. The difficulty of this challenge is to make a comparison of costs/ benefits ratio with traditional products/methods. In fact, manufacturing of TE products currently requires a great number of manual operations performed by trained personnel and has to be compliant with the evolving regulatory framework in terms of Quality Control (QC) and Good Manufacturing Practice (GMP) requirements.

Following this perspective, bioreactors as a means to generate and maintain a controlled culture environment and enabling directed tissue growth could represent the key element for the development of automated, standardized, traceable, cost-effective and safe manufacturing of engineered tissues for clinical applications.

In the following paragraphs, we discuss the role of bioreactors in TE applications, from basic research to streamlined tissue manufacturing processes, highlighting current scientific challenges and future clinical perspectives. In particular, we first review the key functions of bioreactors traditionally employed in research applications as 3D model systems recapitulating aspects of the actual *in vivo* milieu of specific tissues. Afterward we disclose the state of the art in computational modelling of bioreactor systems, and finally we discuss about the basic sensing techniques employed in the engineering of biological tissues to peek inside the "black box" bioreactor. Afterwards, we provide examples, potentials, and challenges of bioreactor-based manufacturing strategies for the production of tissue engineered products for clinical applications.

BIOREACTORS AS 3D *IN VITRO* MODEL SYSTEMS

Through studies of fundamental biology and tissue engineering, we have become increasingly aware that conventional 2D culture systems (i.e. Petri dishes, culture flasks) cannot adequately recapitulate the micro-environment experienced by cells *in vivo*. At the same time, it has become evident that cell differentiation and tissue development *in vivo* are strongly dependent on cell spatial organization and directional cues, and that 3D culture model systems will be vital to gain a greater understanding of basic cell and tissue physiology and pathology within the native *in vivo* micro-environment.

Urged by a rising curiosity in the mechanisms regulating cell metabolism, proliferation and differentiation, as well as cell/cell and cell/material interactions and mechano-transduction dynamics, 3D model systems have been developed to recapitulate specific aspects of the actual *in vivo* milieu of defined tissues (e.g. cartilage, bone, skeletal muscle, bone marrow). These culture systems, besides comprising the appropriate differentiated/undifferentiated cell sources and a proper 3D micro-environment (e.g., scaffolding materials), generally encompass the application of suitable *biochemical* and *physical* cues, resembling the ones sensed by the corresponding tissue *in vivo*. The comprehension of cellular mechanisms is expected to provide the key to achieve a better prediction and control on the bio-mechanical characteristics of the engineered scaffold, as recently proposed by Martin *et al.*[1]

In fact, donor variability, different cell behaviour and incomplete control over the set of physico-chemical variables contribute to make difficult, if not unmanageable, to get a defined threshold of the minimum properties (mechanical and biological) that is necessary to achieve in an engineered graft. To answer the question 'how good is good enough?', bioreactor-based *in vitro* model systems have been used to simulate the behaviour of an engineered graft upon surgical implantation and subsequent exposure to physiological loading regimes.
In one example, engineered cartilage tissues at different developmental stages were exposed to controlled loading regimes resembling a mild post-operative rehabilitation [2]. Results indicated that the response was positively correlated with the amount of glycosaminoglycans in the constructs, suggesting that a more developed engineered tissue could be better suited for early post operative loading after implantation. Reverting the concept, the same experimental setup